**MINISTRY OF EDUCATION AND SCIENCE OF UKRAINE**
Kyiv National University of Construction and Architecture

# SPECIAL ELECTRICAL MACHINES AND ELECTRIC DRIVE IN CONSTRUCTION

Methodological instructions and tasks
to perform calculation and graphic work
for getters of magisteric level of high education
of speciality 141 "Electric power engineering, Electrical Engineering and Electromechanics" specialisation "Electromechanical automation systems"

Kyiv 2024

УДК 621.312.28
C71

Compilers: R. P. Bondar, Doctor of Technical Sciences, Associate Professor;
G.M. Golenkov, Candidate of Technical Sciences, Associate Professor;
O. Volynets, Master's degree
Reviewer S.V. Inosov, Candidate of Technical Sciences, Associate Professor
Responsible for the issue is L.I. Mazurenko, Doctor of Technical Sciences, Professor

*Approved at the meeting of the Department of Electrical Engineering and Electric Drive, protocol № 7 від 23.01.2024 y.*

By the author's editorial team.

C71 Special electric machines and electric drive in construction : methodological instructions for performing calculation and graphic work / compiled by : R.P. Bondar, G.M. Golenkov, O.V. Volynets. – Kyiv : KNUBA, 2024. – 28 p.

The basic methods of calculating the design parameters of electromagnetic, traction and frequency characteristics of a coaxial-linear magnetoelectric motor, vibration drive and electromechanical system in the construction industry are considered.

It is intended for students of speciality 141 "Electric power engineering, electrical engineering and electromechanics".

В авторській редакції.

C71 **Спеціальні** електричні машини та електропривід у будівництві : методичні вказівки до виконання розрахунково-графічної роботи/ уклад. : Р.П. Бондар, Г.М. Голенков, О.В. Волинець. – Київ : КНУБА, 2024. – 28 с.

Розглянуто основні методи розрахунку конструктивних параметрів електромагнітних, тягових та частотних характеристик коаксіально-лінійного магнітоелектричного двигуна, приводу вібраційних та електромеханічних систем у будівництві.

Призначено для здобувачів спеціальності 141 «Електроенергетика, електротехніка та електромеханіка».

## General provisions

The purpose of the calculation and graphic work performed by students in accordance with the norms of the working curriculum in the discipline "Special Electric Machines and Electric Drive in Construction" is to train highly qualified specialists for the construction industry with in-depth knowledge of vibration and electromechanical systems of automated electric drive of construction machines and mechanisms. It also includes theory and practice in the use of special electric machines, in particular, coaxial-linear magnetoelectric motors to drive the working body of electromechanical systems. At the same time, students are required to comprehend the processed scientific and technical literature, study theoretical issues and carry out modelling of electromagnetic, traction and frequency characteristics of drives of electromechanical systems in the construction industry using computer technology.

## Other questions about the practical task:

Start date - 3 weeks; end date - 18 weeks; assignment volume - 30-36 A4 pages; approximate labour intensity - 36...40 hours; students perform the work according to the option (see Table 1) according to the number of the student's record book (first two digits or last two digits). Vibration devices for performing the work are added in accordance with the options.

The design of the calculation and graphic work is carried out in accordance with DSTU 3008: 2015.

## Summary of the practical assignment for the calculation and graphic work

**Theme:**

**Automated electric drive of the vibroelectromechanical system based on ME-CLM for compaction of concrete mix (ME-KLD-CCM).**

1. CALCULATION OF THE DESIGN PARAMETERS OF THE ME-CLD FOR DRIVING THE WORKING BODY OF THE VIBRATING PLATFORM

    1.1 These values are used to calculate the design parameters of a magnetoelectric coaxial linear motor (ME-CLM).

    1.2 The main dimensions of the design and electromechanical parameters of ME-CLM.

2. FREQUENCY CHARACTERISTICS OF THE (ME-CLM-VP)

    2.1 Modelling of frequency characteristics of ME-CLM.

    2.2 Modelling of frequency characteristics of ME-CLM-VP.

CONCLUSIONS

LIST OF REFERENCES

ANNEX

Table 1

**Variants of tasks for the calculation of the magnetoelectric coaxial linear motor ME-CLM**

| № | *P, кVm* | *2p* | *τ, м* | *δ, mm* | cos φ | $\eta_1$, | $A_1', \frac{A}{м}$ | $f_{0.}$, Hz | U, B |
|---|---|---|---|---|---|---|---|---|---|
| 1 | 2 | 3 | 4 | 5 | 6 | 7 | 8 | 9 | 10 |
| **1** | 2,2 | 8 | 0,056 | 1,0 | 0,65 | 0,62 | $30 \cdot 10^3$ | 17 | 220 |
| **2** | 3 | 8 | 0,062 | 1,5 | 0,65 | 0,62 | $30 \cdot 10^3$ | 17 | 220 |
| **3** | 4 | 8 | 0,066 | 1,6 | 0,62 | 0,63 | $30 \cdot 10^3$ | 17 | 220 |
| **4** | 5,5 | 8 | 0,072 | 1,8 | 0,62 | 0,64 | $30 \cdot 10^3$ | 17 | 220 |
| **5** | 7,5 | 10 | 0,076 | 1,8 | 0,62 | 0,65 | $30 \cdot 10^3$ | 17 | 220 |
| **6** | 11 | 12 | 0,080 | 2,0 | 0,65 | 0,65 | $30 \cdot 10^3$ | 17 | 380 |
| **7** | 2,2 | 8 | 0,054 | 1,2 | 0,65 | 0,65 | $32 \cdot 10^3$ | 19 | 220 |
| **8** | 3 | 8 | 0,056 | 1,5 | 0,65 | 0,64 | $32 \cdot 10^3$ | 19 | 220 |
| **9** | 4 | 8 | 0,064 | 1,6 | 0,66 | 0,64 | $32 \cdot 10^3$ | 19 | 220 |
| **10** | 5,5 | 8 | 0,068 | 1,5 | 0,66 | 0,63 | $32 \cdot 10^3$ | 19 | 220 |
| **11** | 7,5 | 8 | 0,072 | 1,6 | 0,66 | 0,65 | $32 \cdot 10^3$ | 19 | 220 |
| **12** | 11 | 10 | 0,074 | 1,8 | 0,65 | 0,66 | $32 \cdot 10^3$ | 19 | 380 |
| **13** | 2,2 | 8 | 0,050 | 1,2 | 0,65 | 0,64 | $32 \cdot 10^3$ | 19 | 220 |
| **14** | 3 | 8 | 0,060 | 1,4 | 0,64 | 0,63 | $32 \cdot 10^3$ | 19 | 220 |
| **15** | 4 | 8 | 0,062 | 1,2 | 0,64 | 0,64 | $32 \cdot 10^3$ | 19 | 220 |
| **16** | 5,5 | 8 | 0,066 | 1,5 | 0,63 | 0,63 | $28 \cdot 10^3$ | 21 | 220 |
| **17** | 7,5 | 10 | 0,068 | 1,8 | 0,65 | 0,65 | $28 \cdot 10^3$ | 21 | 220 |
| **18** | 11 | 12 | 0,076 | 1,6 | 0,66 | 0,64 | $28 \cdot 10^3$ | 21 | 380 |
| **19** | 7,5 | 10 | 0,072 | 1,6 | 0,65 | 0,64 | $28 \cdot 10^3$ | 21 | 220 |
| **20** | 11 | 12 | 0,074 | 1,8 | 0,65 | 0,65 | $28 \cdot 10^3$ | 21 | 380 |
| **21** | 22 | 16 | 0,078 | 2,2 | 0,65 | 0,62 | $28 \cdot 10^3$ | 21 | 380 |
| **22** | 22 | 18 | 0,076 | 2,4 | 0,65 | 0,62 | $31 \cdot 10^3$ | 22 | 380 |
| **23** | 11 | 12 | 0,072 | 1,7 | 0,62 | 0,63 | $31 \cdot 10^3$ | 22 | 380 |
| **24** | 11 | 14 | 0,076 | 1,9 | 0,62 | 0,64 | $31 \cdot 10^3$ | 22 | 380 |

To carry out the calculation and graphic work, we propose the following vibroelectromechanical systems in the construction industry: vibroplatforms for compacting concrete mix (see Table 1, var. 1,6); vibro-devices for pile driving (see Table 1, var. 2,7,13); immersion of reinforcing cages for the formation of injection piles (see Table 1, var. 3,4,8,9); devices for underground utilities (see Table 1, var.5,10), for moving bulk materials (see Table 1, var.18,19); devices for soil compaction (see Table 1, var.12,14,20); vibrating screens (see Table 1, var.16,22); vibrating pumps (see Table 1, var.15,21).

When performing work for all variants:
number of phases $m_1=1$; mains frequency $f=50$ *Hz*; cooling method - ICO141; insulation heat resistance class - F; level of protection against external factors of influence - IP44.

When modelling the electromagnetic and traction characteristics of ME-CLM, an approximated expression [1,2,3,4] for the distribution of magnetic induction in the motor gap was proposed

$$\boldsymbol{B}_{\text{мах}.\boldsymbol{rad}(\boldsymbol{c})} = -\mathbf{0,0338}\boldsymbol{\delta}_{\boldsymbol{rh}} + \mathbf{0,6134}, \quad (1)$$

where $\boldsymbol{\delta}_{\mathbf{rh}}$ is the nonmagnetic gap.

When calculating the values of the parameters of the traction characteristic (Fig. 1.5) F=f(X,I) of the ME-CLM motor [5], we use the approximated expression (2) at a phase voltage of U = 380 V.

$$\boldsymbol{F} \quad = -\mathbf{0,12} * \boldsymbol{X}^{\mathbf{2}} * \boldsymbol{I}_{\boldsymbol{n}} + \mathbf{0,4} * \boldsymbol{X} * \boldsymbol{I}_{\boldsymbol{n}} + \mathbf{19,5} * \boldsymbol{I}_{\boldsymbol{n}}, \quad (2)$$

where $\mathbf{I_n}$ is the rated current in the stator winding of the ME-CLM, A; $\mathbf{X}$ is the movement of the runner (armature), mm (fig. 1.5).

At a phase voltage of U = 220 V, expression (2) takes the form

$$\boldsymbol{F} \quad = (-\mathbf{0,12} * \boldsymbol{X}^{\mathbf{2}} * \boldsymbol{I}_{\boldsymbol{n}} + \mathbf{0,4} * \boldsymbol{X} * \boldsymbol{I}_{\boldsymbol{n}} + \mathbf{19,5} * \boldsymbol{I}_{\boldsymbol{n}})/\sqrt{\mathbf{3}}. \quad \mathbf{(3)}$$

When modelling the characteristics of the magnetic induction distribution [1,2,3,4] in a nonmagnetic air gap $B=f(\delta)$, as well as the electromagnetic traction characteristics $F=f(X,I)$ [5], computer modelling and numerical calculation of the magnetic field in the COMSOL Multiphysic software package were used. The least-squares method and Microsoft Excel software package were used to approximate the maximum values of the parameters of the characteristic curves $B_{max}=f(\delta)$ and $F_{max}=f(X,I)$.

**Theme:**

AUTOMATED ELECTRIC DRIVE OF A VIBROELECTROMECHANICAL SYSTEM BASED ON ME-CLM FOR COMPACTION OF CONCRETE MIX (ME-CLM-CCM).

**(Example)**

## 1. CALCULATION OF THE DESIGN PARAMETERS OF THE ME-CLM FOR DRIVING THE WORKING BODY OF THE VIBRATING PLATFORM

### 1.1 These values are used to calculate the design parameters of a magnetoelectric coaxial linear motor (ME-CLM).

Rated power $P_{nom} = 11kW$;
Phase voltage $U_1 = 380V$;
Number of phases $m_f = 1$;
Weight of the vibrating platform $m_2 = 3000$ kg;
Frequency of the power supply network $f_1$=50 Hz;
ME-CLM natural frequency $f_0$=21 Hz;
Number of poles 2p=12;

Pole distribution $\tau$=0,075 m;

Air gap between stator inductor and runner (secondary element) $\delta = 0{,}015m$;

Previous value of power factor $cos\varphi$=0,65;

Previous value of efficiency $\eta$=0,66;

Preliminary value of the linear load $A_1'=32\cdot10^3$ A/м .

$\alpha_i = \frac{B_{\text{сер.}}}{B'\delta} \approx 0{,}64$ - is the pole overlap coefficient, where the ratio of the average magnetic induction value ($B_{mdl.}$) in the gap to its maximum value ( $B'\delta$) look (1).

The magnetic cores of the stator and the runner (armature) of ME-KLD are made of electrical steel grades E1211; E1213; E320.

## 1.2 The main dimensions of the design and electromechanical parameters of ME-CLM.

Estimated total capacity

$$S_1 = \frac{K_E * P_H}{\eta_1 * cos\varphi} = \frac{0{,}94 * 11000}{0{,}66 * 0{,}65} = 24102{,}6\ \text{VA} = 24\text{kVA}, \qquad (1.1)$$

where $K_E = \frac{E_1}{U_1} = 0{,}94$ while $К_E$ corresponds to a smaller number of pairs (p=3) of poles (according to annex 1.1).

Velocity of the running magnetic field ME-CLM

$$\upsilon_1 = 2\tau f_1 = 2 * 0{,}075 * 50 = 7{,}5 \frac{м}{с}\ . \qquad (1.2)$$

Estimated length of the magnetic circuit of the stator inductor of a magnetoelectric coaxial-linear motor (Fig. 1.1)

$$L_1 = 2\tau p + b_3' = 2 * 75 * 6 + 5{,}5 = 905{,}5\ mm, \qquad (1.3)$$

where $b_3' = (4{,}5 \div 5{,}5)$ – preliminary value of tooth width, mm;

Internal diameter of the stator inductor ME-CLM

$$D_{в1} = \frac{S_1 * 10^6}{\sqrt{2}\pi * К_{об} * \vartheta_1 * L_1 * A_1' * B_б'} = \frac{24{,}103 * 10^6}{\sqrt{2}\pi * 0{,}21 * 7{,}5 * 0{,}905 * 32 * 10^3 * 0{,}6} \approx 200 mm, \qquad (1.4)$$

where $К_{об} = 0{,}21$ installation and design coefficient of the armature runner ME-CLM (0,2÷0,5).

Height of the stator magnetic circuit back

$$h_{c1} = \frac{0{,}5\tau B_б}{k_{c1} B_{c1}} = 0{,}5 * 75 * \frac{0{,}6}{0{,}95 * 1{,}55} = 15 mm, \qquad (1.5)$$

where $k_{c1} = 0{,}95$ – filling factor of the stator magnetic circuit;

$B_b$ is the preliminary calculated value of magnetic induction in the gap using expression (1) $B_{b\text{max}} = -0{,}0338\delta_{rh} + 0{,}6134 = -0{,}0338 * 1{,}5 + 0{,}6134 = 0{,}56\ \text{T}l$, ;

$B_c$ = 1.55 Tl (see Annex 1.2) is the value of magnetic induction of the stator back of the inductor.

Preliminary calculated value of the stator inductor outer diameter

$$D_{c1} = D_{в1} + \tau + 2h_{c1} = 200 + 75 + 2 * 15 = 315\ mm. \qquad (1.6)$$

Preliminary calculated value stator inductor tooth height

$$h_{z1} = \frac{\tau}{2} = \frac{75}{2} = 37{,}5\ mm. \quad (1.7)$$

Number of stator inductor slots

$$Z_1 = m_1 * 2p * q = 1 * 2 * 6 * 5 = 60, \quad (1.8)$$

where q = 5 is the number of grooves per pole. Recommended for pole area within τ = (0.05 - 0.1) m, then the number of grooves per pole (q = 3, 5, 7).

Preliminary gearing of the stator inductor magnetic circuit

$$t_1 = \frac{L_1 - b_{31}}{Z_1} = \frac{905{,}5 - 5{,}5}{60} = 15\ mm. \quad (1.9)$$

Stator inductor tooth width

$$b_{31} = t_1 * \frac{B_б}{k_{c1} * B_{Z1max}} = 15 * \frac{0{,}56}{0{,}95 * 1{,}6} \approx 5\ mm, \quad (1.10)$$

where $B_{Z1max}$ = 1,6 Tl at $Z_1$ = 60 (according to annex 2).

Slot width of the stator inductor magnetic circuit

$$b_{п1} = t_1 - b_{31} = 15 - 5 = 10\ mm. \quad (1.11)$$

Preliminary calculated value of the inner diameter of the stator winding coil

$$D_{bk1} = D_{В1} + 2h_k = 200 + 2 * 2 = 204\ mm, \quad (1.12)$$

where $h_k$ = 2 mm – height of the wedge ring of the stator groove.

The length of the stator magnetic circuit has been revised

$$L_1' = t_1 * Z_1 + b_{31} = 15 * 60 + 5{,}5 = 905\ \text{mm}, \quad (1.13)$$

accept $L_1'$ = 905 mm.

Revised value of the pole distribution stator core length

$$\tau_1' = t_1 * m_1 * q_1 = 15 * 1 * 5 = 75\text{mm}. \quad (1.14)$$

Refined value of the stator running magnetic field velocity

$$\upsilon_1' = 2\tau_1' * f = 2 * 75 * 50 = 7{,}5\ \text{m/s}. \quad (1.15)$$

Height of the slot to be filled with winding

$$h_{п1}' = h_{z1} - h_{k1} = 37{,}5 - 2 = 35{,}5\text{mm}. \quad (1.16)$$

The outer diameter of the magnetic core of the runner (Fig. 1.4), taking into account the gap

$$D_{\text{зм}2} = D_{\text{в}1} - 2\delta = 200 - 2 * 1{,}5 = 197 \text{ mm}. \qquad (1.17)$$

The outer diameter of a permanent magnet (fig. 1.3) is determined by the expression

$$D_{\text{м}} = D_{\text{зм}2} - 2\delta = 197 - 3 = 194 \text{ мм}. \qquad (1.18)$$

Fig. 1.1 shows the design parameters of the ME-CLM stator magnetic circuit.

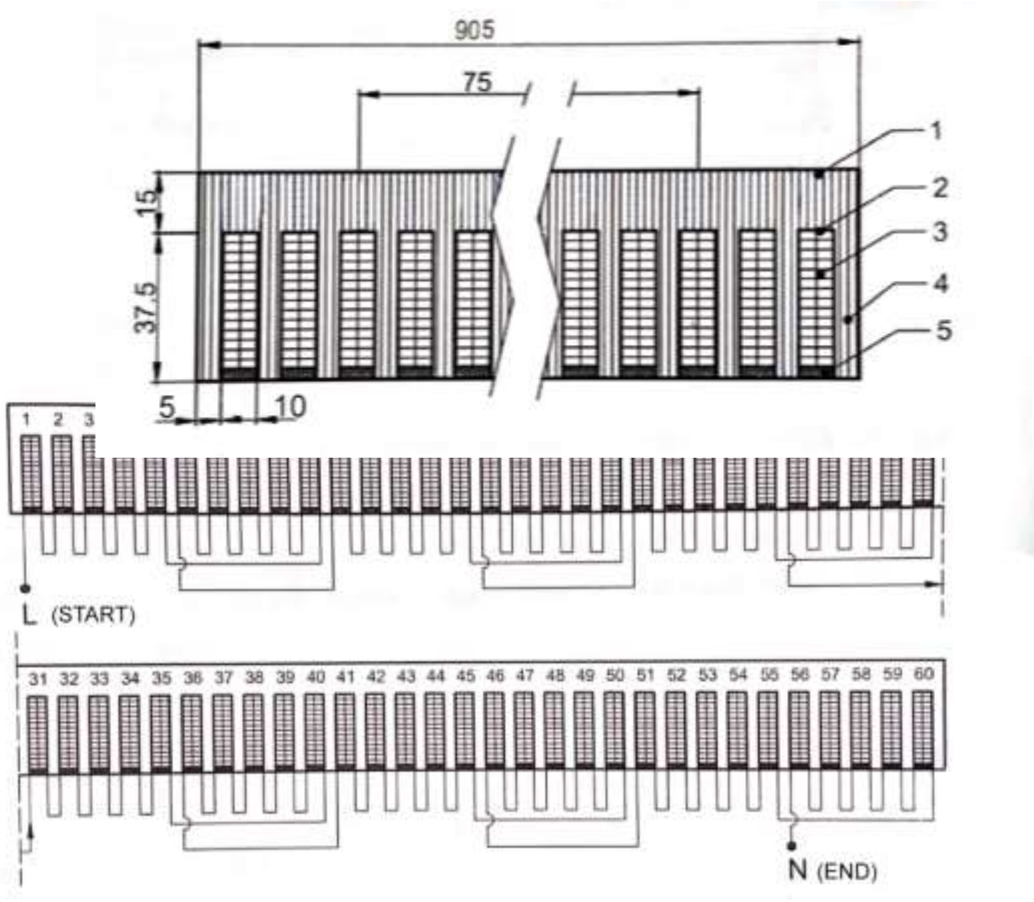


Fig. 1.1 Schematic representation of a stator fragment

1 - magnetic core of the stator inductor; 2 - stator groove; 3 - stator winding (W=420 turns); 4 - stator tooth; 5 - wedge (cylindrical);

**1.3 Calculation of design parameters and stator winding of ME-CLM.**

Winding type. The stator winding of ME-CLM is single-phase.

Fig. 1.2 Diagram of the stator coil winding of ME-CLM (2p = 12 number of poles; $Z_1$=60 - the number of grooves; q = 5 number of grooves (coils) on the pole; W = 420 number of turns in the stator winding)

The current density in the winding is assumed to be $j_1$ = 5,5 A/mm$^2$ (according to annex 1.3).

Preliminary value of the rated phase current in the stator winding

$$I_{п1} = \frac{P_n*10^3}{m_1*U_1*\eta*cos\varphi} = \frac{11*10^3}{1*380*0{,}66*0{,}65} = 68{,}6 \text{ A}. \quad (1.19)$$

Number of effective conductors in the groove

$$N_{п1} = \frac{10^{-3}*A_1'*10^3*t_1*a_1}{I_{1n}} = \frac{10^{-3}*32*10^3*15*2}{68{,}6} = 13{,}99; \quad (1.20)$$

Assume $N_1$ = 14 turns .

Number of consecutive turns in the stator phase winding

$$W_1 = \frac{2pqN_{п1}}{a_1} = 2*6*5*\frac{14}{2} = 420 \text{ turns}. \quad (1.21)$$

Cross-section of an effective conductor in the stator winding

$$q_{1еф} = \frac{I_{1n}}{a_1*j} = \frac{68{,}6}{2*5} = 6{,}86 \text{ мм}^2, \quad (1.22)$$

where j = 5 A/mm$^2$ – current density (according to annex 1.3).

According to (annex 1.4) we take a wire with a rectangular cross-section $q_1$' = 7.137 mm$^2$. Type of conductivity of the conductor. According to DSTU 7013-70, provided that the width of the groove $b_{p1}$ = 9.5 mm. select the conductor a) on the smaller side - $a_{p1}$ = 2 mm; b) on the larger side - $b_{p1}$ = 3.75 mm.

Slot filling factor with insulated conductor

$$k_{зп} = \frac{\sum_1^N S_п}{S_{п1}} = \frac{N_{п1}*q_1*a_1}{h_{п1}'*b_{п1}} = \frac{14*7{,}137*2}{37{,}5*9{,}5} = 0{,}56, \quad (1.23)$$

where $\sum_1^N S_п$ – groove area, mm$^2$.

$S_{п1} = h_{п1} \times b_{п1}$ – groove area, mm$^2$.

Revised value of current density in the stator winding

$$j_1' = \frac{I_{1H}}{a_1*q_1'} = \frac{68{,}6}{2*7{,}137} = 4{,}81 \text{ A/mm}^2. \quad (1.24)$$

Revised value of electromagnetic load

$$A_1' = \frac{I_{1n} * N_{п1} * Z_1}{L_1' * a_1 * 10^{-3}} = \frac{68{,}6*14*60}{905*2*10^{-3}} = 31{,}836 * 10^{-3}\ A/м. \qquad (1.25)$$

Preliminary value of the main magnetic flux

$$\Phi = \frac{k_e * U_{in}}{k_m * f_1 * w_1 k_{об1}} = \frac{0{,}96*380}{1{,}11*50*420*0{,}95} = 0{,}01647\ Vb, \qquad (1.26)$$

where $k_м$ = 1,11 – stator magnetic field shape factor .

Preliminary value of electromagnetic induction

$$B_б' = \frac{2p\Phi}{\alpha * \pi * D_{в1} * L_1' * 10^{-6}} = \frac{2*6*0{,}01647}{0{,}64*3{,}14*0{,}2*0{,}905} = 0{,}544\ \text{Tl}. \qquad (1.27)$$

Choose a NiFeBr magnet with an axial magnetisation vector of cylindrical shape (Fig. 1.3)

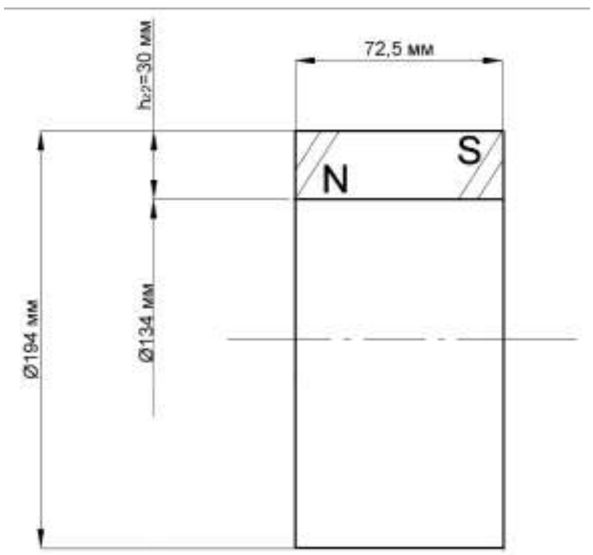


Fig. 1.3 Schematic representation of the ME-KLD runner magnet (armature)

Height of the permanent magnet

$$h_{z2} = 0{,}64 * \tau' * \frac{B_{пм}}{B_{z2}} = 0{,}5 * 75 * \frac{1{,}2}{1{,}9} = 30\ mm, \qquad (1.28)$$

where $B_{пм}$ = 1,2 Tl is the residual induction of an NiFeBr permanent magnet of grade N40; $B_{z2}$ = 1,9 Тл induction of the magnetic field concentrator (pole) of the runner (according to annex 1.2).

The outer diameter of the permanent magnet.

$$b_{\text{пм}} = \tau' - 0{,}5b_{з1} = 75 - 0{,}5 * 5 = 72{,}5\ mm. \quad (1.29)$$

The width of the extreme poles of the armature magnetic flux concentrators (CMP).

$$b_{з2} = \frac{\tau'}{2} = \frac{75}{2} = 37{,}5\ mm. \quad (1.30)$$

The width of the inner pole of the CMP.

$$b_{з3} = \tau' - 0{,}5b_{з1} = 75 - 0{,}5 * 5 = 72{,}5\ mm. \quad (1.31)$$

Then the pole distribution of the runner (armature)

$$\tau_a = 0{,}5 * (b_{\text{пм}} + b_{з3}) = 0{,}5 * (72{,}5 + 72{,}5) = 72{,}5\text{mm}. \quad (1.32)$$

Height of the back of the magnetic core of the runner (armature)

$$h_{c2} = \frac{\alpha \tau B'_б}{B_{c2}} = 0{,}64 * 72{,}5 * \frac{0{,}544}{0{,}85} \approx 30\ mm, \quad (1.33)$$

where $B_{c2}$ = 0,85 – magnetic induction of the back of the runner (armature) Tl.

Armature diameter

$$D_{\text{в}} = D_{\text{зм}2} - 2(h_{z2} + h_{c2}) = 197 - 2 * (30 + 30) = 77\ mm. \quad (1.34)$$

Length of the armature

$$L'_2 = L'_1 * 1{,}4 = 905 * 1{,}4 = 1267\ mm, \quad (1.35)$$

where $К_{\text{мк}}$ = (1,3 – 1,6) installation and design safety factor of the runner length

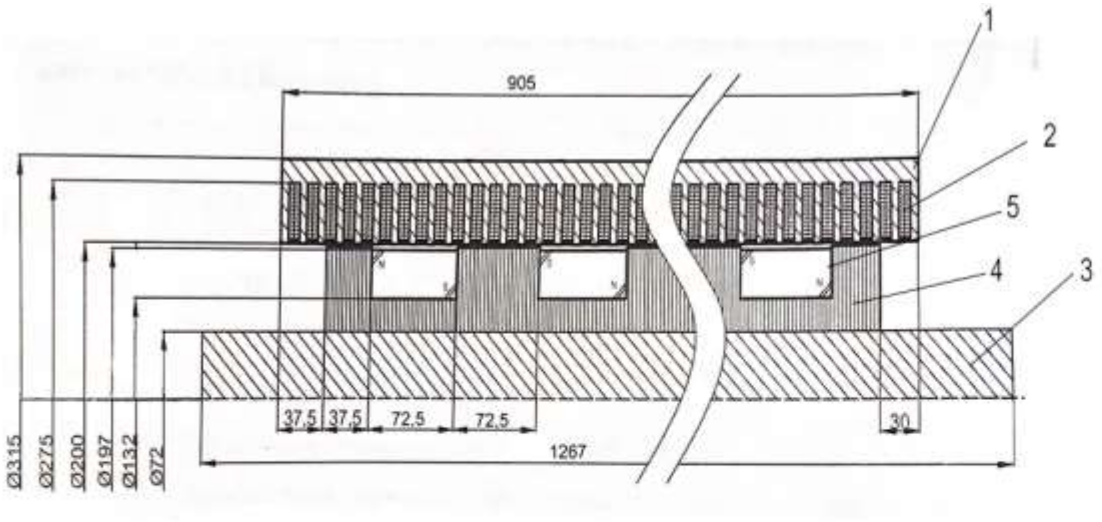


Fig. 1.4 Model of a magnetic-electric coaxial-linear motor.

1 – Stator magnetic circuit ME-CLM; 2 – stator winding; 3 – Runner axis (ME-CLM armature); 4 - pole (magnetic field concentrators) stator of the ME-CLM; 5 – permanent magnets

**Traction characteristics of the ME-CLM**

To calculate the maximum traction value F = f(X) (fig. 1.5) ME-CLM let's use the expression (2):

$$F = -0{,}12 * X^2 * I + 0{,}4 * X * I + 19{,}5 * I, \quad (1.36)$$

where I=68.7 - rated current, A; X - displacement of the runner with a step of 1 mm, within the range (from 0÷7) with mirror image.

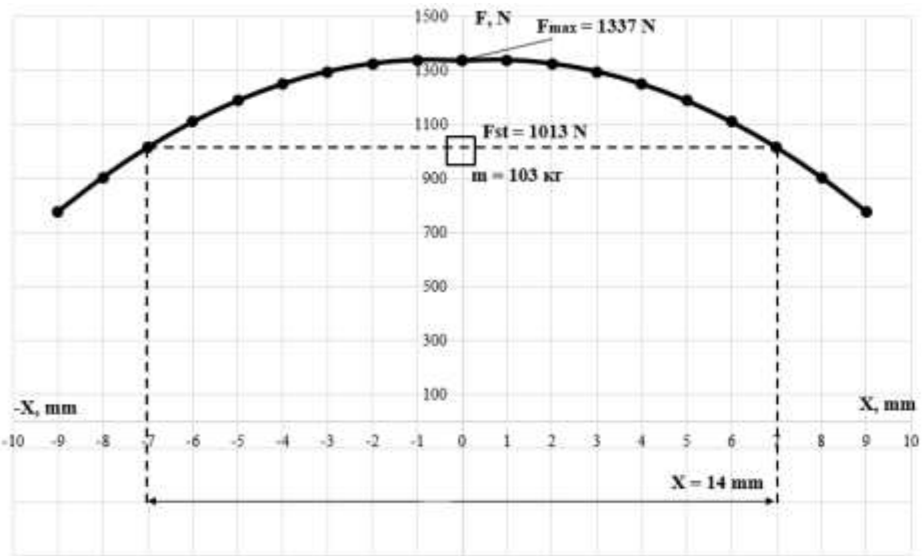


Figure 1.5 Traction characteristic of ME-CLM (P = 11 kW)

The static load Fst is determined by the expression:

$$F_{st} = k_{st}\, F_{a(max)}\ , \quad (1.37)$$

where $k_{st}$ = (0,7 – 0,8 ) – static load factor; $F_{a(max)}$ = 1337 N - the maximum forced traction force developed by the ME-CLM.

The value of the static load coefficient is selected depending on the value of the mass of the moving part of the motor and its amplitude determined by the technological processes, for example: compaction of concrete mix, pile driving, soil compaction, movement of bulk materials, etc.

Analysing existing vibration systems used for compaction of concrete mix in the manufacture of, for example, floor panels, the mass of the static load for these devices is determined by the formula:

In this case, the static mass (mass of the runner with a load) is equal to

$$m_a = F_{st}/g = 1013/9{,}81 = 103\ \text{kg}, \qquad (1.38)$$

where $F_{st}$ = 0,75×1337 = 1013 – static load, N.

Then the amplitude of the runner's oscillation (see Fig. 1.5) with a mass of m = 103 kg moves within X = 14 mm.

# 2. MODELLING OF FREQUENCY CHARACTERISTICS OF AN ELECTROMECHANICAL VIBRATION SYSTEM

## 2.1 Modelling of frequency characteristics of ME-CLM.

The necessity of constructing the amplitude-frequency X = f(f) and the frequency characteristics of the forcing forces F = f(f) of the ME-CLM is determined by the technological task, for example, the quality of the product (panel) when compacting the concrete mix.

The mathematical model of the vibrating electromechanical system (Fig. 2.1) is shown as an equivalent diagram of a vibrating platform for compacting a concrete mixture; the working body is driven by a coaxial-linear magnetoelectric motor (ME-CLM-VP).

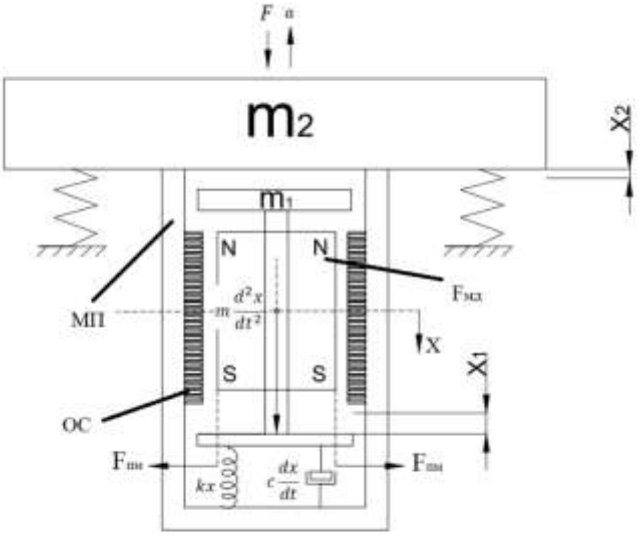


Fig. 2.1 Equivalent kinematic model of a vibrating platform with a magnetoelectric linear drive of the working body

The differential equation of forced oscillations for the ME-CLM vibration system is as follows:

$$m\frac{d^2x}{dt^2}+c\frac{dx}{dt}+kx=F_{a(max)}\cos\omega t+F_{st}, \tag{2.1}$$

where in Fig. 2.1 and in expression (2.1) show the structural components and electromechanical parameters of the ME-CLM-VP: мп - motor stator magnetic circuit; OC - stator winding; NS - permanent magnets; $m_1$ - mass of the moving part of the vibrator (armature), kg; $m_2$ - mass of the vibrating platform, kg; $md^2x/dt^2$ - force applied to the centre of gravity of the moving part of the vibrator (runner), N; $cdx/dt$ - viscous friction force, N; $F_{a(max)}$ - the maximum value of the amplitude of the forcing force; kx - is the tension force developed by the compressed spring, N; $F_{st}$ - the static load; c = $2\pi f0m/Q$ - the coefficient of viscous friction; $f_0$ is the resonant frequency, Hz; X - the displacement of the spring (armature), m; k - the spring stiffness coefficient, N/mm; t - time, sec.

When solving a differential equation, it is necessary to represent expression (2.1) as an equation:

$$\frac{d^2x}{dt^2}+\frac{c}{m}\frac{dx}{dt}+\frac{kx}{m}=\frac{F_{a(max)}}{m}\cos\omega t\pm\frac{F_{st}}{m}, \tag{2.2}$$

Analysing the operation 2.2 with the damping factor taken into account $h=c/2m$ and the natural corner frequency $\omega_0=\sqrt{k/m}$ the equation has the form:

$$\frac{d^2x}{dt^2}+2h\frac{dx}{dt}+\omega_0{}^2x=\frac{F_{a(max)}}{m}\cos\omega t\pm\frac{F_{st}}{m}. \tag{2.3}$$

Then integrate the equation at the initial conditions: $x=x_0$;

$dx/dt=dx_0/dt$, and also at $h<\omega_0$ will be have look:

$$x=e^{-ht}\left(x_0\cos\omega_1 t+\frac{x_0h+x_0}{\omega_1}\sin\omega_1 t\right)-\frac{F_{a(max)}e^{-ht}}{m[(\omega_0^2-\omega^2)^2+4h^2\omega^2]}$$
$$*\left[(\omega_0^2-\omega^2)\cos\omega_1 t+\frac{h}{\omega_1}(\omega_0^2+\omega^2)\sin\omega_1 t\right]+x_a\cos(\omega t-\phi), \tag{2.4}$$

where: $\omega_1=\sqrt{\omega_0^2-h^2}$- precritical resonant frequency, $\varphi$ - is the phase delay of the runner's movement relative to the driving force.

Solving equation (2.1 – 2.4), the expression of the amplitude-frequency response is obtained:

$$x_a=\frac{F_{a(max)}}{m\sqrt{(\omega^2{}_0-\omega^2)^2+4h^2\omega^2}}, \tag{2.5}$$

where: $f_i$ - pre-resonant frequency; $h = \frac{c}{2m} = \frac{F_{max}}{2m*X\omega_0}$ – damping coefficient, $c^{-1}$; $\omega_0 = \sqrt{k/m}$ – where k = 1791410, 443 N/mm$^2$ ; $m_1$ = 103 kg, (see exp. 1.38).

When calculating the amplitude-frequency response *X = f (f)* of the ME-CLM vibration system proposed in this paper, we use expression (2.6) instead of (2.5).

$$X_a = \frac{F_{max}}{m\sqrt{((\omega_0)^2-(2\pi f_i)^2)^2+4h^2(2\pi f_i)^2}} \quad , \qquad (2.6)$$

where: де: $\omega_0 = \sqrt{k/m} = \sqrt{1791410{,}443/103} = 131{,}88$ - the natural angular frequency of the vibrator, $c^{-1}$ ; $\omega_i = 2\pi f_i = 2*3.14*f_i$ is the pre- and post-resonance angular frequency, s-1; when modelling the amplitude-frequency response using expression (2.6), it is calculated within the frequency range $f_i$ = (0-40 Hz) with a step of 1 Hz;the damping coefficient h is used from expression (2.6), when the natural resonant frequency $\omega_0$ is equal to the frequency ω at the maximum value of the amplitude of the forcing force $F_{a(max)}$ and the static load $F_{st}$, then

$$h = \frac{F_{max}}{2m*X\omega_0} = \frac{F_{a(max)}+F_{ст}}{2m*X\omega_0} = \frac{1337+1013}{2*103*0{,}014*2*3{,}14*21} = 6{,}17\ s^{-1}, \qquad (2.7)$$

where $F_{a(max)}$ = 1337 - the maximum value of the motor's driving force , the movement of the runner (1.36), $F_{st}$ = 1013 - static load (1.37), N(look Fig. 1.5); $X_м$ = 0.014 m - the amplitude value of the armature displacement at a mass of $m_1$ = 103 kg (Fig. 1.5).

The calculated parameters of the amplitude-frequency response X = f (f) (Fig. 2.2) of the ME-CLM vibration system are listed in Table 2.1.

Table 2.1 Parameters of the amplitude-frequency response X = f (f)

| f, Hz | 0 | 1 | 2 | 3 | 4 | 5 | 6 | 7 |
|---|---|---|---|---|---|---|---|---|
| X, m | 0,00131 | 0,00131 | 0,00132 | 0,00134 | 0,00136 | 0,00139 | 0,00143 | 0,00147 |
| f, Hz | 8 | 9 | 10 | 11 | 12 | 13 | 14 | 15 |
| X, m | 0,00153 | 0,00161 | 0,00169 | 0,0018 | 0,00194 | 0,00212 | 0,00235 | 0,00265 |
| f, Hz | 16 | 17 | 18 | 19 | 20 | 21 | 22 | 23 |
| X, m | 0,00308 | 0,00372 | 0,00473 | 0,00655 | 0,01019 | 0,01402 | 0,00949 | 0,00585 |
| f, Hz | 24 | 25 | 26 | 27 | 28 | 29 | 30 | 31 |
| X, m | 0,00405 | 0,00304 | 0,00241 | 0,00198 | 0,00167 | 0,00143 | 0,00125 | 0,0011 |
| f, Hz | 32 | 33 | 34 | 35 | 36 | 37 | 38 | 39 |
| X, m | 0,00099 | 0,00089 | 0,00081 | 0,00074 | 0,00067 | 0,00062 | 0,00058 | 0,00053 |

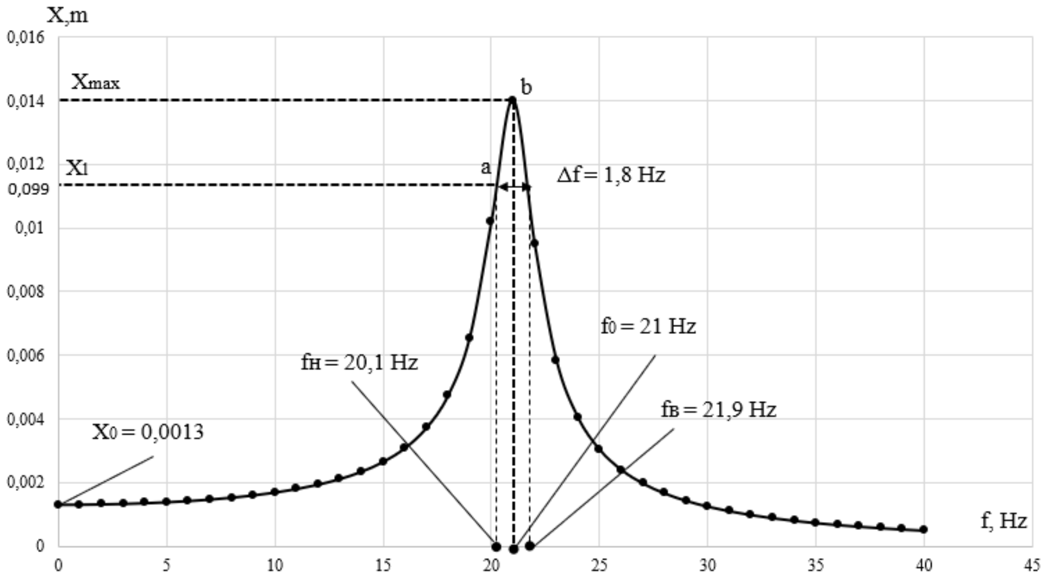


Fig. 2.2 Amplitude-frequency response of X = f(f) of ME-CLM

Analysing the characteristic curve X = f(f) (see Fig. 2.2) shown in the amplitude-frequency response section (a÷b), it characterises the stability of the vibration system. Outside of this section, the system is unstable, so it is recommended to use the operation of this vibration system within the frequency range (20.1 - 21 Hz),where smoothing height $X_l$ skip of the contour Δf is determined by the formula $X_l = X_{max}/\sqrt{2}$ , m.

To calculate the actual value of the parameters of the inertial-force frequency response of the ME-CLM vibration system F=f(f) (Fig. 2.3), the following expression is used:

$$F = m \cdot x \cdot \omega^2, \qquad (2.8)$$

where: $m_1$ = 103 - mass of the runner, kg; - angular frequency = 2πf, $s^{-1}$; X - movement of the runner in the range from 0 to 0.014 mm; f - set frequency of the network, Hz (in the range from 0 to 40 Hz with a step of 1 Hz).

The calculated actual values of the parameter of the inertial-force frequency response $F = f(f)$ of the ME-CLM vibration system are given in table 2.2.

Table 2.2 Parameters of the inertial-force frequency response

| f, Hz | 0 | 1 | 2 | 3 | 4 | 5 | 6 | 7 |
|---|---|---|---|---|---|---|---|---|
| F, N | 0 | 5,34 | 21,5 | 47,95 | 88,45 | 141,18 | 208,8 | 293,56 |
| f, Hz | 8 | 9 | 10 | 11 | 12 | 13 | 14 | 15 |
| F, N | 398,59 | 528,11 | 688 | 886,5 | 1135,8 | 1453,71 | 1868,3 | 2425,4 |
| f, Hz | 16 | 17 | 18 | 19 | 20 | 21 | 22 | 23 |
| F, N | 3205,9 | 4363,9 | 6229,3 | 9609,5 | 16551,3 | 25114,9 | 18654 | 12556,4 |
| f, Hz | 24 | 25 | 26 | 27 | 28 | 29 | 30 | 31 |
| F, N | 9465,7 | 7712,2 | 6605,7 | 5850 | 5303,6 | 4891,5 | 4570,3 | 4313,5 |
| f, Hz | 32 | 33 | 34 | 35 | 36 | 37 | 38 | 39 |
| F, N | 4103,8 | 3929,7 | 3783 | 3657,8 | 3550 | 3456,2 | 3373,9 | 3301,3 |

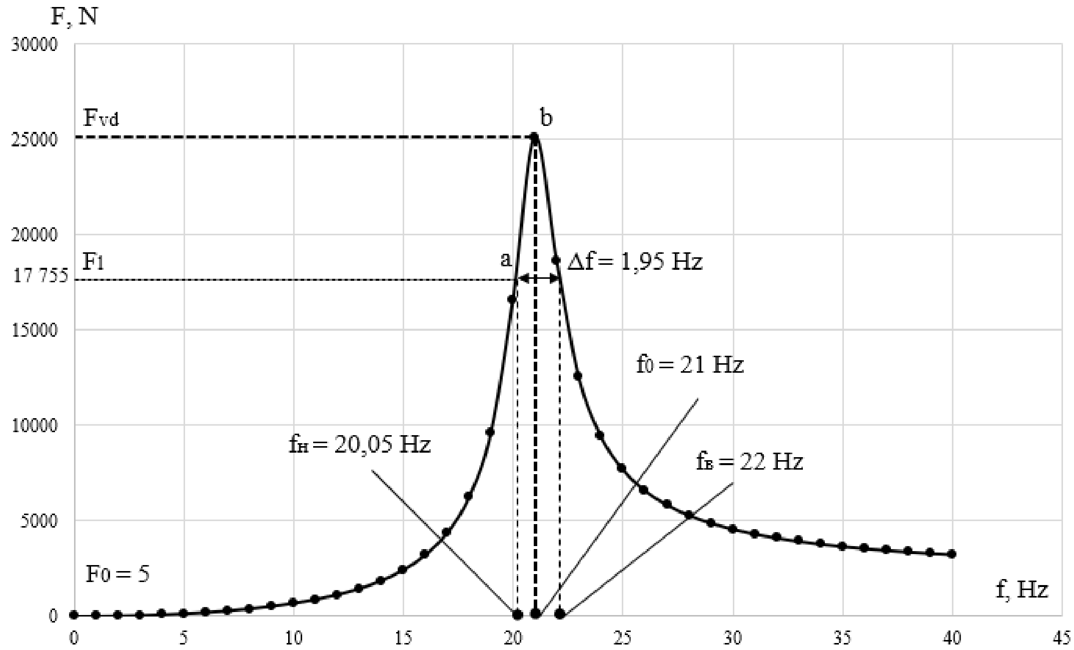


Fig. 2.3 Frequency response of the electromechanical vibration system ME-CLM:

Analysing the characteristic curve F = f(f) (see Fig. 2.3) shown in the frequency response section (a÷b), it characterises the stability of the vibration system. Outside of this section, the system is unstable, so it is recommended to use the operation of this vibration system within the frequency range (20.05 - 21 Hz).

### 2.2 Modelling of frequency characteristics of ME-CLM-VP.

To determine the amplitude of oscillations of the vibration system ME-CLM-VP weighing 3103 kg, provided that the natural frequencies of the vibration systems ME-CLM and ME-CLM-VP coincide, the amplitude value of the electromechanical vibration system (ME-CLM-VP) weighing 3103 kg is calculated by the expression:

$$X_{vp} = \frac{\mathrm{F_{vd}}}{\mathrm{m_{vp}}\omega_0^2} = \frac{25114}{3103*17392} \approx 0{,}00046\ \text{м} = 0{,}46\ \text{мм}\ , \qquad (2.10)$$

where $F_{vd}$ = 25114 is the actual value developed by the ME-CLM motor at the maximum oscillation amplitude, N (see Fig. 2.3).

The damping coefficient for this vibration system ME-CLM-VP is determined by the formula:

$$h_{\text{вп}} = \frac{\mathrm{F_{a(max)}+F_{st}}}{2\mathrm{m_{vp}}*\mathrm{X_{vp}}\omega_0} = \frac{2350}{2*3103*0{,}00046*131{,}88} = 6{,}2\ \text{с}^{-1}, \qquad (2.11)$$

where: $m_{vp}$ = 3103 - mass of the vibrating platform, kg; $X_{vp}$ = 0.00046 - amplitude value of the ME-CLM-VP vibration system, m.

The parameters of the frequency response $X_{vp}$ = f(f) were calculated using formula (2.12) within the frequency range $f_0$ = (0 - 40) Hz with a step of 1 Hz:

$$x_{вп} = \frac{F_{a(max)}}{m_{вп}\sqrt{({\omega^2}_0-\omega^2)^2+4h_{вп}^2\omega^2}}, \qquad (2.12)$$

where $h_{vp}$ = 6.2 is the damping coefficient, $s^{-1}$ (2.11).

The calculated parameters of the amplitude-frequency response X = f (f) (Fig. 2.4) of the ME-CLM-VP vibration system are listed in Table 2.3.

Table 2.3 Parameters of the amplitude-frequency response of the ME-CLM-VP

| f, Гц | 0 | 1 | 2 | 3 | 4 | 5 |
|---|---|---|---|---|---|---|
| X, м | 0,0000435 | 0,0000436 | 0,0000439 | 0,0000445 | 0,0000451 | 0,0000461 |
| f, Гц | 6 | 7 | 8 | 9 | 10 | 11 |
| X, м | 0,0000473 | 0,0000489 | 0,0000508 | 0,0000532 | 0,0000562 | 0,0000598 |
| f, Гц | 12 | 13 | 14 | 15 | 16 | 17 |
| X, м | 0,0000644 | 0,0000702 | 0,0000778 | 0,000088 | 0,0001023 | 0,000123 |
| f, Гц | 18 | 19 | 20 | 21 | 22 | 23 |
| X, м | 0,000157 | 0,000217 | 0,000337 | 0,000463 | 0,000314 | 0,000193 |
| f, Гц | 24 | 25 | 26 | 27 | 28 | 29 |
| X, м | 0,000134 | 0,0001 | 0,0000798 | 0,0000655 | 0,0000552 | 0,0000475 |
| f, Гц | 30 | 31 | 32 | 33 | 34 | 35 |
| X, м | 0,0000414 | 0,0000366 | 0,0000327 | 0,0000294 | 0,0000267 | 0,0000244 |
| f, Гц | 36 | 37 | 38 | 39 | 40 | 41 |
| X, м | 0,0000223 | 0,0000206 | 0,000019 | 0,0000177 | 0,0000165 | 0,0000154 |

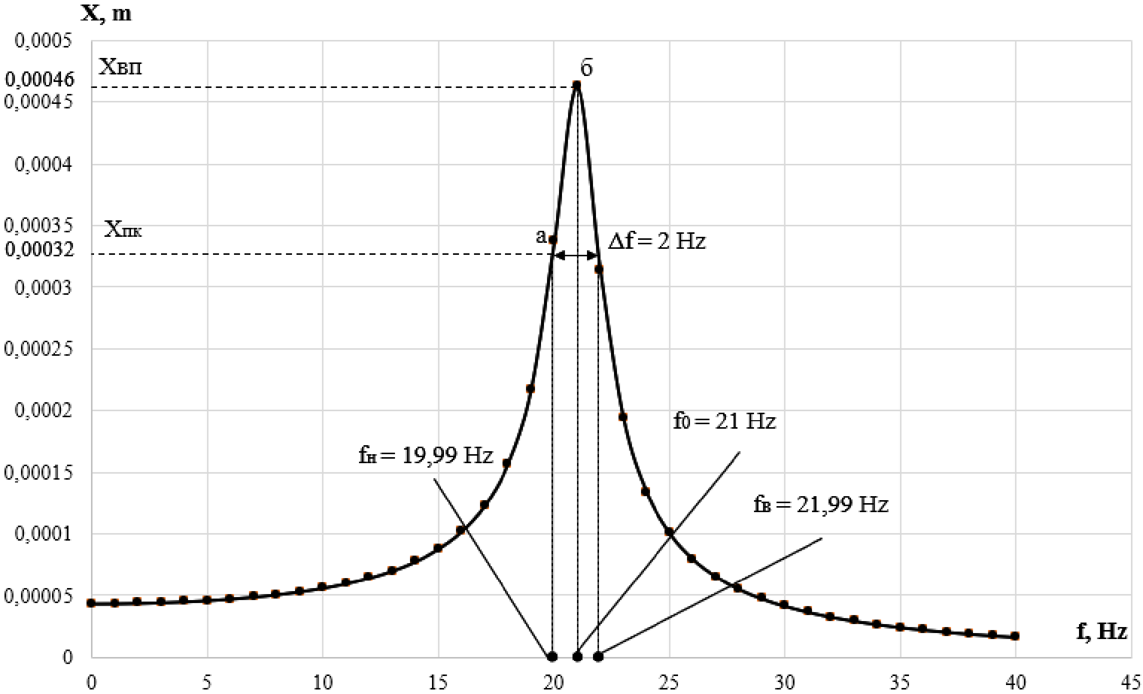

Fig. 2.4 Amplitude-frequency response of the vibration system ME-CLM-VP

It is recommended that the operation of the ME-CLM-VP vibration system, in the dynamic mode, be performed within the limits (a÷b) of the amplitude-frequency response, frequencies f = (19.99 - 20.99) Hz.

## Conclusion.

The analysis has shown that the results of modelling and calculation of traction and frequency characteristics in the dynamic mode of operation of the vibration system based on a magnetoelectric coaxial-linear motor, at resonance $f_0$ = 21 Hz and at the maximum value of the vibration amplitude of the vibration platform X = 0.46 mm, the actual value of the inertial force developed by the ME-CLM with a power of P = 11 kW is **$F_{di}$ = 25114 N.** Thus, the use of the ME-CLM-VP system allows for the technological process of compacting concrete mix for floor panels and other concrete products with minimal energy consumption and reliability compared to other types of vibration systems.

## Schematic diagram of connection of ME-CLM-CCM with a frequency converter

In the experimental study of the amplitude-frequency characteristics of the ME-KLD-VP vibration system, it is proposed to use a frequency converter of two-phase systems.

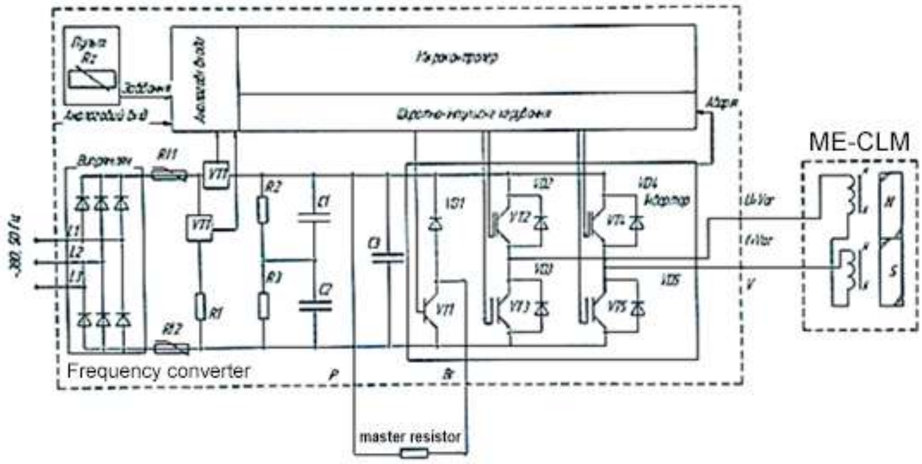


Fig. 2.5 shows the block diagram of the frequency converter inclusion in the ME-CLM-VP system.

Fig. 2.5 Principle wiring diagram of ME-CLM-VP.

For example, for this vibration system ME-CLM-VP, it is proposed to use a Delta Electronics frequency converter (Table 2.1).

Table 2.1. Technical characteristics of the Delta Electronics frequency converter.

| | |
|---|---|
| Power | 22 kW |
| Number of phases/input voltage | 3-p/380 (three-phase 380V) |
| Number of phases/output voltage | 3-p/380 V |
| Mmax (1 min) % | 110-130 |
| Rated current | 90.00 A |
| Maximum output frequency | 400 Hz |
| Degree of IP protection | 20 |
| Built-in regulator | PID |
| Number/type of analogue inputs | 3(1: 0-10V; 2: 0-10V or 0(4)-20mA) |
| Number of discrete inputs | 2 |
| Number of relay outputs | 3 |
| Nominal resistance | 5 kOhm |
| ModBus TCP/IP protocol | CMC-MOD01 |
| CANopen protocol | CMC-MOP01 |
| PROFIBUS DP protocol | CMC-PD01 |
| Ethernet IP protocol | CMC-EIP01 |

The power part of the converter consists of an output rectifier, a DC link, an inverter and a control system. The input rectifier is made according to the Larionov circuit. The rectifier is connected to the DC link, which consists of thermistors Rt1 and Rt2 and large-capacity electrolytic capacitors C1 and C2. Thermistors with a negative temperature coefficient are used to limit the charging current when the converter is switched on. When cold, thermistors have a high resistance. After the inverter is switched on, the current flowing through the thermistors heats them up, which causes them to sharply reduce their resistance. In this way, the thermistors limit the charging current of the capacitors, and in the process of operation they have virtually no effect on the voltage of the capacitors.

Capacitors C1 and C2 smooth the DC link voltage, filter the current consumed from the mains, provide reactive energy return to the motor when the inverter is switched on and during transients, and provide energy return during frequency braking of the CLM. Resistors R2 and R3, connected in parallel to each capacitor, charge them.

The output of the DC link is connected to a left-phase voltage inverter, which consists of two half bridges on transistors VT2-VT5 and a brake switch on transistor VT1 with a reverse diode VD1. If necessary, a braking resistor is connected to the brake key, which will dissipate energy in the frequency braking mode of the motor. Reverse diodes VD2-VD5 are used to transfer energy from the motor to the power supply. These diodes conduct whenever the direction of current is opposite to the direction of the inverter input voltage. Thus, the voltage inverter allows for the bidirectional flow of both energy and current.

## CONCLUSIONS

The structural and electromechanical traction characteristics of the working body based on the ME-CLM of the electromechanical vibration system obtained as a result of the calculation allow this method of calculating the structural and electromechanical characteristics of the ME-CLM to be used in the development of the drive of various working bodies of electromechanical vibration systems. For example, compaction of concrete mix in the forming of reinforced concrete products; devices for pile driving, destruction of oversized material, immersion of metal pipe, soil compaction, devices for underground utilities, movement of various bulk materials, etc.

## LIST OF SOURCES

1. Голенков Г.М., Аббасян М. Дослідження розподілу електромагнітної індукції в зазорі лінійного синхронного двигуна// Наука, освіта і практика. Наукове видання. – Кременчук: КНУ, 2011. Вип. 1/2011(1). – С. 254-256

2. Голенков Г.М., Аббасян М., Розподіл магнітної індукції в повітряному зазорі коаксіально-лінійного синхронного двигуна з аксіальним і радіальним напрямком намагнічування постійних магнітів на бігуні. // Електротехніка і електромеханіка//. Харків. – 2012. – №2 – С. 30-32.

3. Голенков Г.М., Аббасян М., Розподіл магнітної індукції в повітряному зазорі коаксіально-лінійного синхронного двигуна з аксіальним і радіальним напрямком намагнічування постійних магнітів на бігуні. // Електротехніка та електромеханіка. Харків. – 2013. – №1 – С. 16-21.

4. Голенков Г.М., Аббасян М., Моделювання розподілу магнітної індукції коаксіально-лінійного двигуна з аксіальним і радіальним напрямком намагнічування постійних магнітів. // Електротехніка і електромеханіка. Харків. – 2014. – №1 – С. 21-25.

5. Голенков Г.М., Аббасян М., Електромеханічні характеристики - лінійного двигуна з аксіальним і радіальним напрямками намагнічування постійних магнітів. //Технічна електродинаміка. – 2014. – №3 – С. 64-69.

6. Голенков Г.М., Аббасян М., Моделювання роботи коаксіально-лінійних двигунів з аксіальним і радіальним напрямками намагнічування за допомогою постійних магнітів при динамічному режимі. // Електротехніка та електромеханіка. Харків. – 2014. – №6 – С. 21-29.

7. Лінійні магнітоелектричні двигуни вібраційної дії для приводу будівельних машин і механізмів. Монографія/ Р.П. Бондар, Г.М. Голенков, О.Д. Подольцев – К.: Інститут електродинаміки НАН України. 2021 – 274 с.

# ANNEX

## Annex 1.1

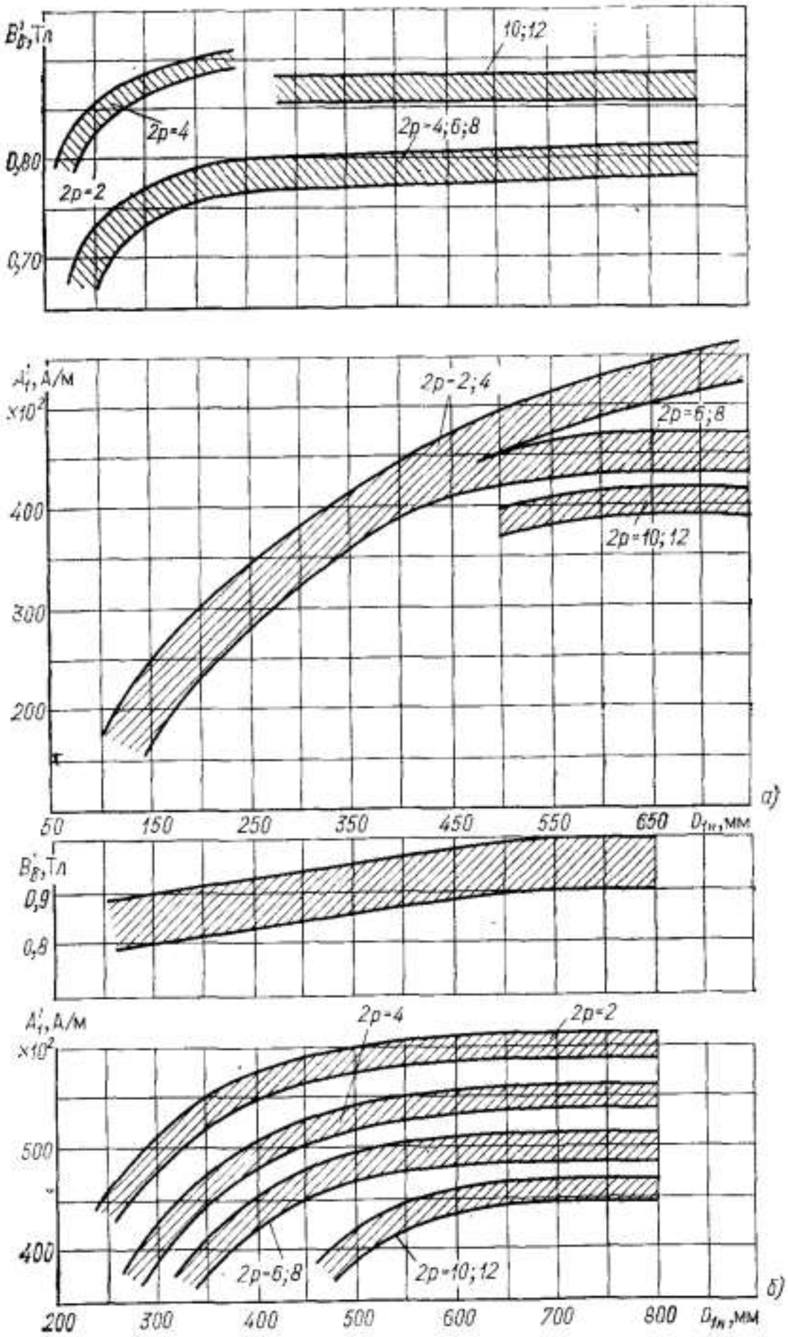

# Annex 1.2

| $h$, mm | $2p$ | Stator slot shape | Stator winding type | Recommended values of magnetic induction, Tl. when motors are designed according to the method of protection IP 44. | |
|---|---|---|---|---|---|
| | | | | $B_{z1max}$ | $B_{C1}$ |
| 50—132 | 2, 4 | Trapezoidal | Single-layer bulk | 1,75—1,95 | 1,50—1,65 |
| | 6 | | | 1,75—1,95 | 1,45—1,60 |
| | 8 | | | 1,70—1,90 | 1,20—1,35 |
| 160 | 2 | Trapezoidal | Two-layer bulk | 1,75—2,0 | 1,45—1,70 |
| | 4 | | Single-layer bulk | 1,75—2,0 | 1,45—1,70 |
| | 6 | | The same | 1,70—1,85 | 1,35—1,50 |
| | 8 | | | 1,70—1,85 | 1,10—1,20 |
| 180—250 | 2, | Trapezoidal | Two-layer bulk | 1,70—1,90 | 1,45—1,65 |
| | 4, 6 | | One-two-layer in bulk | 1,70—1,90 | 1,45—1,65 |
| | 8 | | Two-layer bulk | 1,70—1,85 | 1,10—1,20 |
| 280—355 | 2, 4, 6, 8 | Rectangular half-open | Two-layer rigid half-coils | 1,70—1,90 | 1,40—1,60 |
| | 10 | Trapexoidal half-open | Two-layer concentric in bulk | 1,60—1,80 | 1,30—1,45 |
| | 12 | The same | The same | 1,60—1,80 | 1,15—1,30 |

## Annex 1.3

| Name | Material: Name, brand | Material: Thickness, mm | No. of layers |
|---|---|---|---|
| Groove box | Polyethylene terephthalate film | 0,19*<br>0,25* | 1<br>1 |
| Groove cover | The same | 0,25*<br>0,35* | 1<br>1 |
| Gasket mcphase in frontal parts | Film-asbocardboard | 0,35 | 1 |
| Insulation of in-machine connections and lead ends | Insulation tube | — | — |
| Frontal bandage | Polyester thread | — | — |
| Impregnation | Lacquer ML-92 or compound KP-34 | — | — |
| Coating of frontal parts | Enamel GF-92-GS | — | — |

* For motors with $h = 50 \div 63$ мм.
** For motors with $h = 71 \div 132$ мм.

## Annex 1.4

| Nominal wire size on the larger side b, mm | Nominal wire size on the smaller side a, mm: 0,80 | 0,85 | 0,90 | 0,95 | 1,00 | 1,06 | 1,12 | 1,18 | 1,25 | 1,32 | 1,40 | 1,50 | 1,60 | 1,70 | 1,80 | 1,90 | 2,00 | 2,12 |
|---|---|---|---|---|---|---|---|---|---|---|---|---|---|---|---|---|---|---|
| | Design wire cross-section, mm² | | | | | | | | | | | | | | | | | |
| 2,00 | 1,463 | 1,545 | 1,626 | 1,706 | 1,785 | 1,905 | 2,025 | 2,145 | 2,285 | 2,425 | 2,585 | — | — | — | — | — | — | — |
| 2,12 | 1,559 | — | 1,734 | — | 1,905 | — | 2,160 | — | 2,435 | — | 2,753 | — | — | — | — | — | — | — |
| 2,24 | 1,655 | 1,749 | 1,842 | 1,934 | 2,025 | 2,160 | 2,294 | 2,429 | 2,585 | 2,742 | 2,921 | 3,145 | 3,369 | — | — | — | — | — |
| 2,36 | 1,751 | — | 1,950 | — | 2,145 | — | 2,429 | — | 2,735 | — | 3,089 | — | 3,561 | — | — | — | — | — |
| 2,50 | 1,863 | 1,970 | 2,076 | 2,181 | 2,285 | 2,435 | 2,585 | 2,736 | 2,910 | 3,085 | 3,285 | 3,535 | 3,785 | 3,887 | 4,137 | — | — | — |
| 2,65 | 1,983 | — | 2,211 | — | 2,435 | — | 2,753 | — | 3,098 | — | 3,495 | — | 4,025 | — | 4,407 | — | — | — |
| 2,80 | 2,103 | 2,225 | 2,346 | 2,466 | 2,585 | 2,753 | 2,921 | 3,089 | 3,285 | 3,481 | 3,705 | 3,985 | 4,265 | 4,397 | 4,677 | 4,957 | 5,237 | — |
| 3,00 | 2,263 | — | 2,526 | — | 2,785 | — | 3,145 | — | 3,535 | — | 3,985 | — | 4,585 | — | 5,038 | — | 5,638 | — |
| 3,15 | 2,383 | 2,522 | 2,661 | 2,799 | 2,935 | 3,124 | 3,313 | 3,502 | 3,723 | 3,943 | 4,195 | 4,510 | 4,825 | 4,992 | 5,307 | 5,622 | 5,937 | 6,315 |
| 3,35 | 2,543 | — | 2,841 | — | 3,135 | — | 3,537 | — | 3,973 | — | 4,475 | — | 5,145 | — | 5,667 | — | 6,337 | — |
| 3,55 | 2,703 | 2,862 | 3,021 | 3,179 | 3,335 | 3,548 | 3,761 | 3,974 | 4,223 | 4,471 | 4,755 | 5,110 | 5,465 | 5,672 | 6,027 | 6,382 | 6,737 | 7,163 |
| 3,75 | 2,863 | — | 3,201 | — | 3,535 | — | 3,985 | — | 4,473 | — | 5,035 | — | 5,785 | — | 6,387 | — | 7,137 | — |
| 4,00 | 3,063 | 3,245 | 3,426 | 3,606 | 3,785 | 4,025 | 4,265 | 4,505 | 4,785 | 5,065 | 5,385 | 5,785 | 6,185 | 6,437 | 6,837 | 7,237 | 7,637 | 8,117 |
| 4,25 | 3,263 | — | 3,651 | — | 4,035 | — | 4,545 | — | 5,098 | — | 5,735 | — | 6,585 | — | 7,287 | — | 8,137 | — |
| 4,50 | 3,463 | 3,670 | 3,876 | 4,081 | 4,285 | 4,555 | 4,825 | 5,095 | 5,410 | 5,725 | 6,085 | 6,535 | 6,985 | 7,287 | 7,737 | 8,187 | 8,637 | 9,177 |
| 4,75 | 3,663 | — | 4,101 | — | 4,535 | — | 5,105 | — | 5,723 | — | 6,435 | — | 7,385 | — | 8,188 | — | 9,137 | — |
| 5,00 | 3,863 | 4,095 | 4,326 | 4,556 | 4,785 | 5,085 | 5,385 | 5,685 | 6,035 | 6,385 | 6,785 | 7,285 | 7,785 | 8,137 | 8,637 | 9,137 | 9,637 | 10,24 |
| 5,30 | 4,103 | — | 4,596 | — | 5,085 | — | 5,721 | — | 6,410 | — | 7,205 | — | 8,265 | — | 9,177 | — | 10,24 | — |
| 5,60 | 4,343 | 4,605 | 4,866 | 5,126 | 5,385 | 5,721 | 6,057 | 6,393 | 6,785 | 7,177 | 7,625 | 8,185 | 8,745 | 9,157 | 9,717 | 10,28 | 10,84 | 11,51 |
| 6,00 | 4,663 | — | 5,226 | — | 5,785 | — | 6,505 | — | 7,285 | — | 8,185 | — | 9,385 | — | 10,44 | — | 11,64 | — |

## Notes

Educational and methodological publication

**SPECIAL ELECTRICAL MACHINES AND ELECTRIC DRIVE IN CONSTRUCTION**

Methodological instructions and tasks
to perform calculation and graphic work
for getters of magisteric level of high education
of speciality 141 "Electric power engineering, Electrical Engineering and Electromechanics" specialisation "Electromechanical automation systems"

Compilers: Roman **BONDAR,**
Gennadiy **GOLENKOV,**
Oleksandr **VOLYNETS**

Випусковий редактор *Л. С. Тавлуй*
Комп’ютерне верстання *Д. М. Ніколаєвич*

Підписано до друку 17.05.2024. Формат 60 x 84 1 /16
Ум. друк. арк. 1,63. Обл.-вид. арк. 1,75.
Електронний документ. Вид. № 108/ІІІ-24

Видавець і виготовлювач:
Київський національний університет будівництва і архітектури

Проспект Повітряних Сил, 31, Київ, Україна, 03037

Свідоцтво про внесення до Державного реєстру суб’єктів
видавничої справи ДК № 808 від 13.02.2002